

# 1 Two-Dimensional Simulation

## 1.1 State

A simulation is considered complete when it can predict the state  $X$  of the drone for the next discrete time segment.

$$X = [z, y, \phi, \dot{z}, \dot{y}, \dot{\phi}] \quad (1)$$

The state  $X$  consists of the coordinates on the z-axis, which points positively towards the center of the Earth, the y-axis, and the vector  $\phi$ , which describes the rotation angle about the x-axis. Additionally, the velocities, i.e., the rates of change,  $\dot{z}, \dot{y}, \dot{\phi}$  of these quantities are also part of the vector.

The thrust  $F_1$  and  $F_2$  of the two rotors, in combination with environmental influences, produce all forces that result in changes to the state vector  $X$ .

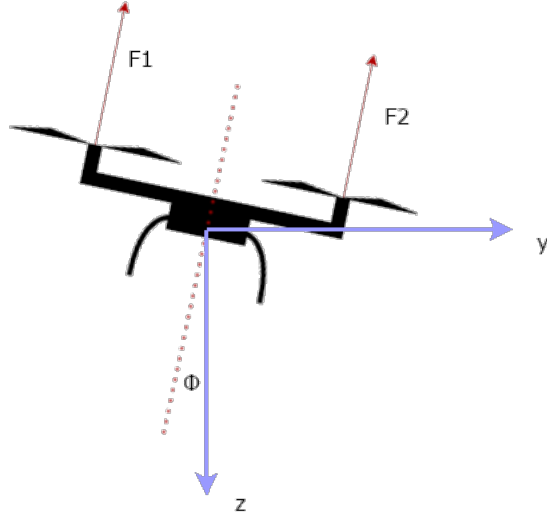


Figure 1: Two-dimensional drone

The thrusts  $F_1$  and  $F_2$  are directed at an angle  $\phi$  to the z-axis.

## 1.2 Dynamics

Dynamics describe how the state  $X$  changes based on  $F_1$  and  $F_2$ . To work with fundamental quantities,  $F_1$  and  $F_2$  are expressed by their underlying rotor velocities  $\omega_1$  and  $\omega_2$ . The relationship  $k_f$  between rotor velocity and force is quadratic as shown in [1, S. 4]. Hence, we have:

$$F_i = k_f \omega_i^2 \quad (2)$$

This relationship  $k_f$  is determined experimentally as explained in Chapter 3. The changes in state in the positions  $z$ ,  $y$ , and  $\phi$  result from the integration of the velocities  $\dot{z}$ ,  $\dot{y}$ , and  $\dot{\phi}$ . The state changes of these result from the integration of the accelerations  $\ddot{z}$ ,  $\ddot{y}$ , and  $\ddot{\phi}$ . These are derived from  $F = ma$  and the force of gravity  $F_g = mg$  with  $g = 9.81 \frac{m}{s^2}$ :

$$\ddot{z} = \frac{F_g - F_z}{m} = g - F_z \quad \ddot{y} = \frac{F_y}{m} \quad (3)$$

$F_z$  is parallel to the z-axis, and  $F_y$  is parallel to the y-axis. Thus, there is a right angle between  $F_z$  and  $F_y$ . Additionally, it holds true that

$$F_{total} = \sum_1^i F_i = F_1 + F_2 \quad (4)$$

The total force of both rotors  $F_{total}$  is oriented at an angle  $\phi$  to the z-axis.

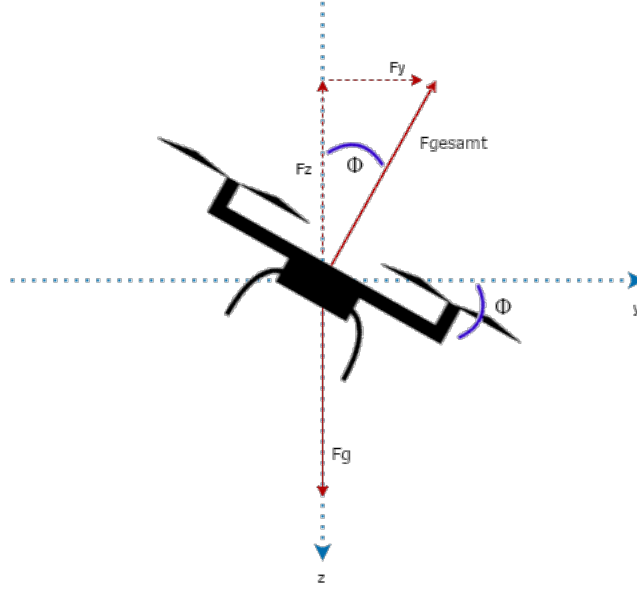


Figure 2: Forces on a 2D drone

Thus, the forces  $F_z$  and  $F_y$  result from the triangle's trigonometry as

$$F_z = F_{total} \cos \phi \quad F_y = F_{total} \sin \phi \quad (5)$$

and the accelerations along the z- and y-axes by combining Equations 1.2, 1.2, and 1.2:

$$\ddot{z} = g - \frac{(F_1 + F_2) \cos \phi}{m} \quad \ddot{y} = \frac{(F_1 + F_2) \sin \phi}{m} \quad (6)$$

$\ddot{\phi}$  is derived through the combination of the equations for torque  $M$ .  $l$  is the distance from the center of mass of the dual-rotor drone to one of the motors.

$$M_x = F_\phi l \quad M_x = I_x \ddot{\phi} \quad (7)$$

The moment of inertia  $I_x$  has to be determined experimentally, as described in Chapter 3. The force around the x-axis  $F_\phi$  is the difference in the two motor forces  $F_1$  and  $F_2$  from Figure 1. A positive  $F_\phi$  corresponds to clockwise rotation, and a negative value indicates counter-clockwise rotation. In summary, we have:

$$F_\phi = F_1 - F_2 \quad (8)$$

Therefore, the angular acceleration  $\ddot{\phi}$  can be described as

$$\ddot{\phi} = \frac{(F_1 - F_2) \cdot l}{I_x} \quad (9)$$

Hence, the dual-rotor drone's state at time  $t$  can be determined by the sum of the state  $X(t)$  and the integral of the time derivative of the state  $\dot{X}$ .

$$X(t + \Delta t) = X(t) + \int_t^{t+\Delta t} \dot{X}(\tau) d\tau \quad (10)$$

## 2 Three-Dimensional Simulation

### 2.1 State

In the three-dimensional case, the state vector  $X$  consists of twelve quantities and is formally defined as

$$X = [x, y, z, \phi, \theta, \psi, \dot{x}, \dot{y}, \dot{z}, p, q, r] \quad (11)$$

where

$x, y, z$  represent positions,

$\dot{x}, \dot{y}, \dot{z}$  represent velocities in their respective axes,

$\phi, \theta, \psi$ , also known as Euler angles, represent rotations about the x-axis, y-axis, and z-axis, and

$p, q, r$  are the angular velocities about the axes  $kx$ ,  $ky$ , and  $kz$  in the body coordinate system.

Except for the last three parameters, all information resides in the world coordinate system, which was the only one used in the two-dimensional case from Chapter 2. The body coordinate system, however, is a fixed coordinate system attached to the quadrotor.

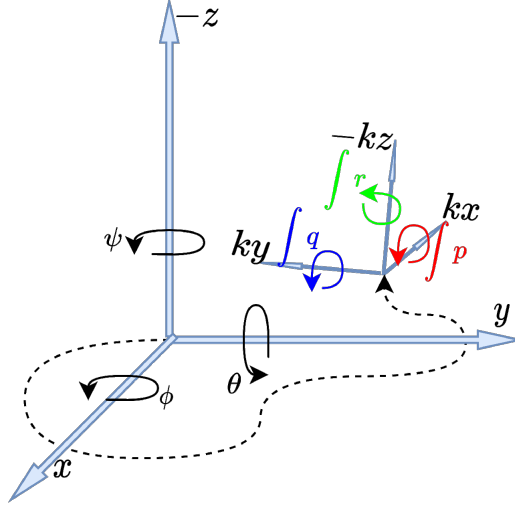


Figure 3: World and body coordinate systems

## 2.2 Dynamics

Equation (1.2) still applies here as before. Analogous to Equation 1.2, in the three-dimensional case, we also require the derivative  $\dot{X}$  of the state vector to move the state forward in time. Equations 1.2 still apply but now, analogous to  $\ddot{y}$ , we add the formula for  $\ddot{x}$ . In summary, still derived from Newton's  $F = ma$ , we have

$$\ddot{z} = \frac{F_g - F_z}{m} = g - F_z \quad \ddot{y} = \frac{F_y}{m} \quad \ddot{x} = \frac{F_x}{m} \quad (12)$$

Different from the two-dimensional case, however, are the formulas for  $F_x$ ,  $F_y$ , and  $F_z$ . Here a rotation matrix is defined [2, S. 12], which transforms any vector from the body coordinate system into a vector in the world coordinate system through multiplication. Essentially, the matrix is still based on triangle trigonometry. The matrix  $R_{Body}^{World}$  is

$$\begin{aligned} & \begin{bmatrix} 1 & 0 & 0 \\ 0 & \cos(\phi) & -\sin(\phi) \\ 0 & \sin(\phi) & \cos(\phi) \end{bmatrix} \begin{bmatrix} \cos(\theta) & 0 & \sin(\theta) \\ 0 & 1 & 0 \\ -\sin(\theta) & 0 & \cos(\theta) \end{bmatrix} \begin{bmatrix} \cos(\psi) & -\sin(\psi) & 0 \\ \sin(\psi) & \cos(\psi) & 0 \\ 0 & 0 & 1 \end{bmatrix} \\ &= \begin{bmatrix} c(\psi)c(\theta) & c(\psi)s(\theta)s(\phi) - s(\psi)c(\phi) & s(\psi)s(\phi) + c(\psi)s(\theta)c(\phi) \\ s(\psi)c(\theta) & c(\psi)c(\phi) + s(\psi)s(\theta)s(\phi) & s(\psi)s(\theta)c(\phi) - c(\psi)s(\phi) \\ -s(\theta) & c(\theta)s(\phi) & c(\theta)c(\phi) \end{bmatrix} \end{aligned} \quad (13)$$

So, from Equations 2.2 and 2.2, we derive the formulas for axis accelerations

in the world coordinate system as

$$\begin{bmatrix} \ddot{x} \\ \ddot{y} \\ \ddot{z} \end{bmatrix} = \begin{bmatrix} 0 \\ 0 \\ g \end{bmatrix} + \frac{1}{m} R_{Body}^{World} \begin{bmatrix} 0 \\ 0 \\ -F_{total} \end{bmatrix} = \begin{bmatrix} R_{13} \frac{1}{m} (-F_{total}) \\ R_{23} \frac{1}{m} (-F_{total}) \\ g + R_{33} \frac{1}{m} (-F_{total}) \end{bmatrix} \quad (14)$$

Here it is also shown that the propellers generate thrust in the direction  $-kz$ . On Earth,  $g = 9.81 \frac{m}{s^2}$ . And the total force now results from the sum of all four rotors, so that

$$F_{total} = \sum_1^i F_i = F_1 + F_2 + F_3 + F_4 \quad (15)$$

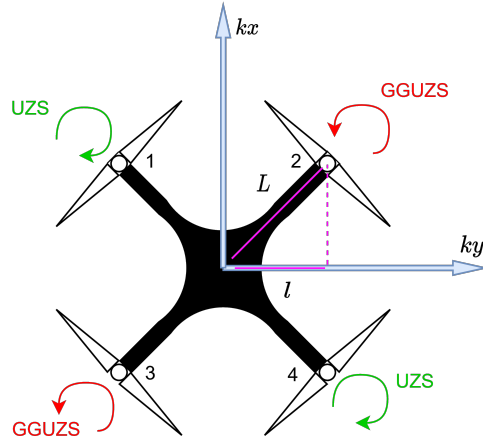


Figure 4: 3D Drone from above: Propeller rotation directions and numbers.  $kz$  goes into the plane of the drawing.

The accelerations around the body axes  $\dot{p}$ ,  $\dot{q}$ , and  $\dot{r}$  are calculated by the Euler's equation of motion, which is

$$\begin{aligned} M &= I\dot{\omega} + \omega \times (I\omega) = \\ \begin{bmatrix} M_x \\ M_y \\ M_z \end{bmatrix} &= \begin{bmatrix} I_x & 0 & 0 \\ 0 & I_y & 0 \\ 0 & 0 & I_z \end{bmatrix} \begin{bmatrix} \dot{p} \\ \dot{q} \\ \dot{r} \end{bmatrix} + \begin{bmatrix} p \\ q \\ r \end{bmatrix} \times \left( \begin{bmatrix} I_x & 0 & 0 \\ 0 & I_y & 0 \\ 0 & 0 & I_z \end{bmatrix} \begin{bmatrix} p \\ q \\ r \end{bmatrix} \right) \end{aligned} \quad (16)$$

The moments of inertia  $I_x$ ,  $I_y$ , and  $I_z$  are determined by experiments, as explained in Chapter 3. By rearranging, we then get the accelerations as

$$\begin{aligned}
\begin{bmatrix} M_x \\ M_y \\ M_z \end{bmatrix} &= \begin{bmatrix} I_x & 0 & 0 \\ 0 & I_y & 0 \\ 0 & 0 & I_z \end{bmatrix} \begin{bmatrix} \dot{p} \\ \dot{q} \\ \dot{r} \end{bmatrix} + \begin{bmatrix} qI_x r - rI_y q \\ rI_x p - pI_z r \\ pI_y q - qI_x p \end{bmatrix} \\
\begin{bmatrix} M_x - (qI_x r - rI_y q) \\ M_y - (rI_x p - pI_z r) \\ M_z - (pI_y q - qI_x p) \end{bmatrix} &= \begin{bmatrix} I_x & 0 & 0 \\ 0 & I_y & 0 \\ 0 & 0 & I_z \end{bmatrix} \begin{bmatrix} \dot{p} \\ \dot{q} \\ \dot{r} \end{bmatrix} \\
\begin{bmatrix} \dot{p} \\ \dot{q} \\ \dot{r} \end{bmatrix} &= \begin{bmatrix} \frac{1}{I_x} & 0 & 0 \\ 0 & \frac{1}{I_y} & 0 \\ 0 & 0 & \frac{1}{I_z} \end{bmatrix} \begin{bmatrix} M_x - (qI_x r - rI_y q) \\ M_y - (rI_x p - pI_z r) \\ M_z - (pI_y q - qI_x p) \end{bmatrix} \\
\begin{bmatrix} \dot{p} \\ \dot{q} \\ \dot{r} \end{bmatrix} &= \begin{bmatrix} \frac{M_x - r q (I_x - I_y)}{I_x} \\ \frac{M_y - r p (I_x - I_z)}{I_y} \\ \frac{M_z - p q (I_y - I_x)}{I_z} \end{bmatrix}
\end{aligned} \tag{17}$$

As remaining necessary quantities to establish  $\dot{X}$ , which is the goal in dynamics, we have the velocities about the world coordinate system axes  $\dot{\phi}$ ,  $\dot{\theta}$ , and  $\dot{\psi}$ . These are obtained, like the linear accelerations in Equation 2.2 with the help of a rotation matrix specifically for Euler angle velocities [3, S. 12, Eq. 79]

$$\begin{bmatrix} \dot{\phi} \\ \dot{\theta} \\ \dot{\psi} \end{bmatrix} = \begin{bmatrix} 1 & \sin(\phi) \tan(\theta) & \cos(\phi) \tan(\theta) \\ 0 & \cos(\phi) & -\sin(\phi) \\ 0 & \sin(\phi)/\cos(\theta) & \cos(\phi)/\cos(\theta) \end{bmatrix} \begin{bmatrix} p \\ q \\ r \end{bmatrix} \tag{18}$$

Thus, the state of the quadrotor at time  $t$  can be determined by the sum of the state  $X(t)$  and the integral of the state's derivative  $\dot{X}$ .

$$X(t + \Delta t) = X(t) + \int_t^{t+\Delta t} \dot{X}(\tau) d\tau \tag{19}$$

### 3 Determination of Simulation Parameters

In addition to the laws of dynamics, some central quantities also determine the behavior of the quadrotor. These are

$m$  the mass,

$k_f$  the constant for the quadratic relationship between rotor velocity and thrust,

$k_m$  the constant for the quadratic relationship between rotor velocity and torque,

$I_x, I_y, I_z$  the moments of inertia about each axis.

These constants must be determined experimentally.  
The mass is measured with a bathroom scale. A project member weighs himself and then again while holding the drone near his upper body. The difference gives the mass  $m$ .  
 $k_f$  and  $k_m$  are measured using a seesaw.

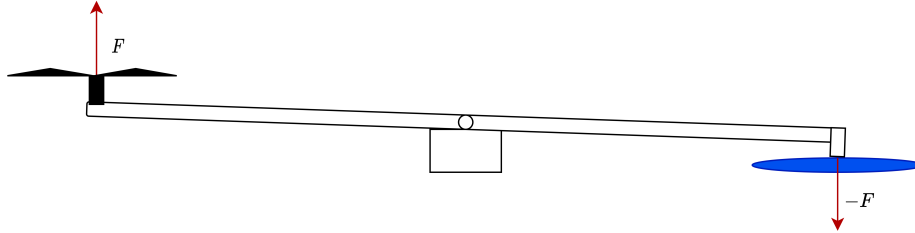


Figure 5: Diagram of Seesaw: Measurement of  $k_f$ . The kitchen scale is colored blue.

At one end, the propeller is attached, and at the other end, a pin pushes the thrust force onto a kitchen scale. By reading the weight on the scale, the resulting force can be determined.



Figure 6: Photo of Seesaw: Measurement of  $k_f$

$k_m$  can be measured with a slight modification of the seesaw. The propeller simply needs to stand at a  $90^\circ$  angle to the seesaw.



Figure 7: Photo of Seesaw: Measurement of  $k_m$

The rotational velocity is recorded by a tachometer. To this end, a reflective

strip is attached to the propeller. The tachometer emits a laser and counts the number of reflections per minute.



Figure 8: Photo Tachometer: Measurement of  $\omega$  with a tachometer

Measured $v$ [rads/s]	Measured $k_f$ [N]	Measured $k_m$ [N]
20.00	0.56898	0.11772
26.70	0.99081	0.30411
35.08	1.74618	0.37278
41.26	2.43288	0.6867
48.17	3.2373	0.981
53.20	4.08096	1.12815
58.85	4.93443	1.30473
62.41	5.4936	1.52055
65.97	6.0822	1.6677

Table 1: Results of Experiments

The test series yielded a  $k_f = 0.00141446535$  and a  $k_m = 0.0004215641$ . The moments of inertia are dependent on the weight and dimensions of the drone body. This paper uses results from a publication in which a similar frame of reference was used.[4, S. 7] Thus we have  $I_x = 0.0121$ ,  $I_y = 0.0119$ , and  $I_z = 0.0223$ .



## References

- [1] F. I. T. Johansen Tor and S. Berge, “Constrained Nonlinear Control Allocation with Singularity Avoidance using Sequential Quadratic Programming,” *IEEE Transactions on Control Systems Technology*, vol. 12, no. 1, pp. 211–216, 2004.
- [2] L. F. L. Johnson Eric N. and S. B. L, *Aircraft Control and Simulation: Dynamics, Controls Design, and Autonomous Systems*. New Jersey: Wiley-Blackwell, 2015.
- [3] D. James, “Representing Attitude: Euler Angles, Unit Quaternions, and Rotation Vectors,” *self*, 2006.
- [4] N. Xuan-Mung and S.-K. Hong, “Improved altitude control algorithm for quadcopter unmanned aerial vehicles,” *Applied Sciences*, vol. 9, no. 10, 2019.